Sensor Calibration through Load Tests at the Digital Bridge Schwindegg

M.Eng. Johannes Wimmer *
Dipl.-Ing. Christian Kainz **
M.Sc. Diego Mediel-Cuadra ***
M.Sc. Esther Simisi ****
M.Sc. Rhena Schütz *****
M.Sc. Philipp Radusch ******
M.Sc. Eid Rezaie *******
Dr.-Ing. Stefan Küttenbaum ********
Prof. Dr.-Ing. Thomas Braml *********

* University of the Bundeswehr Munich, Institute of Structural Engineering, Germany, johannes.wimmer@unibw.de
** University of the Bundeswehr Munich, Institute of Structural Engineering, Germany, christian.kainz@unibw.de
**** University of the Bundeswehr Munich, Institute of Structural Engineering, Germany, diego.mediel@unibw.de
**** Former Student of the University of the Bundeswehr Munich, Germany, esther.simisi@unibw.de
***** Former Student of the University of the Bundeswehr Munich, Germany, rhena.schütz@unibw.de
****** Bundeswehr, Bonn, Germany, philippradusch@bundeswehr.org
******* Former Student of the University of the Bundeswehr Munich, Germany, eid.rezaie@unibw.de
******** University of the Bundeswehr Munich, Institute of Structural Engineering, Germany, stefan.kuettenbaum@unibw.de
********* University of the Bundeswehr Munich, Institute of Structural Engineering, Germany, thomas.braml@unibw.de

Abstract:
Sensors are indispensable information sources for our intelligent world. In transport infrastructure, manifold sensors are utilized to monitor structure, traffic, and environment. These systems may be combined in digital twins. The sensors are installed for defined tasks, such as temperature and crack monitoring, modal analyses, deformation and traffic load monitoring. Weigh-in-motion or bridge weigh-in-motion systems are used to determine the axle loads. However, if the traffic load on the bridge is to be determined, a few strain sensors may be sufficient. To do so, the measured strains must be assigned to different loads, which means that the sensors must be calibrated. An extensive test program was carried out on the digital bridge in Schwindegg with three trucks of different weights to calibrate the bridge's strain sensors. Static tests with stationary loads and dynamic crossing tests at different speeds showed which sensors are well suited to which areas of the bridge and which are poorly suited to this type of monitoring.

Keywords: Structural Health Monitoring, Calibration Test, Sensor, Finite Element Analysis

1 Introduction

In an increasingly digitalized and automated world, many opportunities arise to make use of these advanced technologies. According to the Report on the state of the Digital Decade 2023, which is published by the European Commission, Germany is in the European midfield in terms of digitalization [1]. Furthermore, a digitalization index is published within Germany, in which the degree of digitalization of the various business sectors is depicted [2]. The construction industry scores poorly here, despite current developments towards digital construction planning, e.g. with building information modeling (BIM). Efforts are also being made to digitize bridge structures, but these are usually only sufficient for digitization and not for real digitalization. Digitization involves converting documents into a digital format, but without using the document for data-driven analyses. Digitalization, on the other hand, describes the conversion of analogue information into a processable digital form [3].

One promising method of digitalization is the data-driven structural assessment utilizing measurement methods such as non-destructive testing (NDT) or sensors. These techniques are used to measure short-term or long-term impacts and the effects of environments on assets. Their applications are still mostly isolated cases. The reasons for this are costs, labor and skill shortages in construction and metrological research needs in order to provide easily applicable methods yielding comparable measurement results. However, as the built environment continues to age, there is a discernible trend towards implementing additional monitoring systems, testing new measurement methods and, in particular, driving forward the digitalization of transport infrastructure. One approach to this is to carry out measurements to determine traffic loads in order to evaluate the real-time utilization of the bridge.

This paper provides insights into a monitoring research project emphasizing the preparations for a traffic load monitoring on a medium-span prestressed concrete road bridge. In the next chapter 2, the applied methods, namely Structural Health Monitoring (SHM), Bridge load tests, determination of traffic load using sensors and stress and strain evaluation using Finite Element Analysis (FEA) are introduced. In the following third chapter, a test procedure for calibrating sensors is presented using the digital bridge Schwindegg as case study and then discussed in chapter 4.

2 State of the art

2.1 Structural Health Monitoring on bridge structures

In damage detection, Farrar and Worden distinguish between NDT, SHM, condition monitoring (CM) and statistical process control (SPC) [4]. NDT describes a measurement in which damage is a priori suspected or even detected and localized at a certain point [4]. CM and SHM methods are used to detect such damage. The principles are identical, CM is used when rotating machines are involved. With SPC, the focus is not on the structure, but on the processes. For this reason, the bridge inspection and monitoring strategy developed in the present study is based on SHM and NDT.

SHM also differentiates between the duration of the monitoring measure. Short-time monitoring is limited to a few minutes to days, e.g. in the case of a test load. Long-time monitoring is conducted over a longer time period, which can last several weeks, months or even years. Permanent monitoring means monitoring until the end of the structure's life. As already described in [5], "for structures, a permanent surveillance from the beginning to the end of the lifetime is not common. Monitoring is mostly used as a so-called emergency monitoring to secure the usability and until the bridge can be repaired or replaced. [...] The monitored details are those where the damage occurred." However, the first pilot projects in which monitoring systems were already installed during construction are already being implemented [5],[6].

The usual procedure for carrying out such an SHM is the use of sensors. Depending on the (expected) damage pattern and the evaluation method used, different measurement procedures and evaluation methods are used. A wide range of sensors and monitoring methods have been developed for this purpose, for example modal analyses with accelerometers [7], deformation measurements with displacement sensors or traffic load determination with strain sensors [8].

2.2 Bridge load tests

Bridge load testing remains a vital tool in structural engineering, particularly when analytical methods are insufficient to capture a structure's actual performance under realistic conditions. Originally used to demonstrate the safety of new bridges to the public [9], load tests today are primarily applied to existing structures, especially when construction plans are unavailable [10],[11], materials have degraded [12], or retrofitting measures must be validated [13],[14]. A notable example is the *Elbe Bridge* in Bad Schandau, Germany, where large scale load tests were conducted in 2025 following a full closure due to suspected damage. These tests were essential to assess the structural capacity under real loading scenarios before deciding on a possible reopening [15].

Load tests are generally categorized into diagnostic, proof, and acceptance tests [16]. Diagnostic tests, performed under service level loads, are designed to monitor sensor responses and validate analytical or numerical models [17]. These tests include both static load tests (e.g., with parked vehicles, suspended weights, or distributed loads such as sandbags or concrete blocks) and dynamic load tests (with controlled vehicle crossings), enabling the assessment of structural linearity, load distribution, and sensor stability [18]. A representative example is the *Vahrendorfer Stadtweg* Bridge in Hamburg, Germany, where diagnostic tests were used to validate over 100 sensors and calibrate a finite element model under both static and dynamic loading conditions [19]. Proof load tests, in contrast, subject the bridge to loads close to design limits to verify safety [20]. Acceptance tests are conducted on newly built bridges to confirm regulatory compliance and establish a reference state. For instance, the *Reallabor Intelligente Brücke* at the Autobahn junction Nuremberg, Germany was instrumented immediately after construction and subjected to targeted vehicle crossings to generate baseline data for long-term monitoring [21].

In the context of sensor evaluation and SHM, both static and dynamic load tests offer complementary and distinct advantages. Static tests are particularly effective for assessing slow structural responses and long-term signal stability. They enable the calibration and verification of strain gauges under quasi-constant loading conditions and are especially suited for evaluating linearity, sensor drift, and temperature compensation. Dynamic tests, on the other hand, are more suitable for analyzing transient structural behavior, damping characteristics, and frequency-dependent effects. They also provide insight into the reproducibility of sensor responses during controlled vehicle movements [19]. In Germany, the technical framework for conducting load tests on concrete structures is provided by the DAfStb guideline [22], which distinguishes between suitability, control, and proof tests. Additional practical considerations are described by Bretschneider et al. [23], who emphasize that diagnostic tests using regular heavy vehicles can be a realistic and efficient alternative to laboratory-like test setups, as long as the applied loads do not exceed the serviceability limit state (SLS).

2.3 Determination of traffic load using sensors

Traffic loads can be determined in different ways. The methods differ in the use of sensors. A trending method is the Bridge Weigh-in-Motion (B-WiM). It enables the determination of vehicle loads under moving traffic to derive object-specific traffic load models. A distinction is made between direct and indirect measurement methods [24]. Direct systems work with plate or strip sensors in the road pavement, while indirect systems use strain and displacement measurements on the bridge superstructure [24],[25]. The latter offer advantages in terms of durability and robustness, but require more complex evaluations.

Indirect systems primarily use strain gauges, vibrating wire or fiber optic sensors. Sensors are usually positioned centrally on the underside of bridge beams. In addition, temperature measuring devices (e.g. thermocouples, thermistors) are used to filter out temperature-related deformations [25]. Filter algorithms are essential for data

processing in order to separate traffic influences from temperature and noise components. The speed and total weight of a vehicle are recorded by global sensors, while axle spacing and axle loads are identified by local sensors [8],[26],[27]. Genetic algorithms, artificial neural networks and reference influence lines are used for this purpose [24].

Calibration tests with known vehicle data are used for system validation and FE model adaptation. Furthermore, they facilitate the establishment of realistic limit values and load assumptions. Furthermore, vehicle identification considers lateral distributions due to laterally offset sensors. Object-specific load models are derived from the collected traffic data [28]. These are used for recalculation in accordance with applicable guidelines. The approval of the highest road construction authority is required, particularly for the application of higher recalculation levels. Extreme value distributions can also be used to make probabilistic statements about maximum loads and failure probabilities - crucial for a realistic safety assessment and load-bearing capacity estimation of bridge structures. Other methods use laser scanners and webcams, for example. These can be used to measure traffic by detecting and counting vehicles. Information on vehicle type, dimensions, speed and lanes is stored and evaluated. In addition, traffic jams can be recorded [26]. 2D LiDAR sensors or IoT webcams are used, for example.

2.4 Stress and strain evaluation using Finite Elements Analysis

In the context of stress and strain evaluation, the strain on the underside of the cross-section under the TS (tandem system) needs to be determined. The internal forces from the TS and other relevant internal forces were calculated using the FEA. For prestressed concrete bridges, an uncracked condition is assumed. In this state reinforced concrete and prestressed concrete cross-sections generally behave in a linear-elastic manner, with concrete and reinforcing steel jointly participating in the absorption of tensile stresses. Apart from the force introduction areas, where part of the force is transferred to concrete via the composite mechanisms, there is an even distribution of strain and thus also of stresses in concrete and steel. In this case, ideal composite behavior is assumed [29].
The linear relationship between strain and stress is defined as the Young's modulus, which is derived from following equations:

$$\varepsilon = \frac{\sigma_c}{E_c} \tag{1}$$

$$\sigma_c = \frac{M}{W_y} + \frac{N}{A_c} \tag{2}$$

In practical bridge design, mostly linear elastic calculation and material parameters are used to determine stress in the SLS. A realistic calculation of the stress-strain or deformation state in the bridge components is therefore limited for the following reasons:

- complexity of the geometry and load distribution in longitudinal and transversal direction
- difficulty in formulating boundary conditions (e.g. soil bedding, stiffness of additional components like asphalt)
- nonlinearity of the material behavior

The results from a calculation model are necessary to link the reaction of the bridge under the actual traffic to a load model, e.g. LM 1 according to EN 1991-2 [30]. Depending on the type of the used element type, e.g. beam, shell or brick elements, a deviation in the internal forces of up to 15% can be observed under identical material parameters and load conditions [31]. Further variation in the results is introduced from the stiffness of connection points, e.g. frame corner, and the modulus of subgrade reaction. Code regulations often give guidance for the safe assessment of the load bearing capacity of structures. However, this is not identical to the actual load bearing behavior of the structure. As a result, it is recommended to maintain a single modeling approach and, based on this model, to determine the strains or internal forces resulting from both the calibration vehicle and the normative load model.

3 Use case of the digital bridge Schwindegg (Germany)

3.1 Introduction of bridge and sensors

In the Bavarian/German district of Mühldorf am Inn, a district road bridge was replaced in 2022 as part of a new construction project. The bridge is in a suburb of Schwindegg and crosses the river Isen with a span of approx. 21.7 m. The bridge consists of prestressed prefabricated beams with cast-in-place concrete supplements. The bridge structure is designed as a frame, the abutments are founded on bored piles. The integral structure has the special feature that sensors were already installed in the structure during the construction of the bridge. For this purpose, the sensor planning was already carried out during the planning phase of the structure and the detailed planning was already carried out with the tender and the structural design. This meant that 140 sensors, which provide 170 independent measurement data, could be installed without delaying the construction process. The power and internet connection created on the bridge in the specially provided technical block ensures almost uninterrupted recording of the measurement data since the opening to traffic in December 2022.

The sensors, which include strain gauges, inclinometers, accelerometers, earth pressure sensors, water level gauges, vibrating wire gauges and temperature sensors, were installed and attached at the most meaningful locations. The sensors were measured using tachymeters, 3D laser scans and trilateration [32]. The finite element model of the bridge

was used to determine strains, deformations, inclinations, natural shapes and natural frequencies. The measurement tasks considered were the recording of the actual passing traffic, the analysis of structural strains due to seasonal temperature influences on the integral structure, the interaction of the abutment with the bored piles and the stiffness of the frame corner [5]. This work's relevant sensors and their positions in the cross section are shown in Figure 1. Further information about this project can be found in [5],[6],[32].

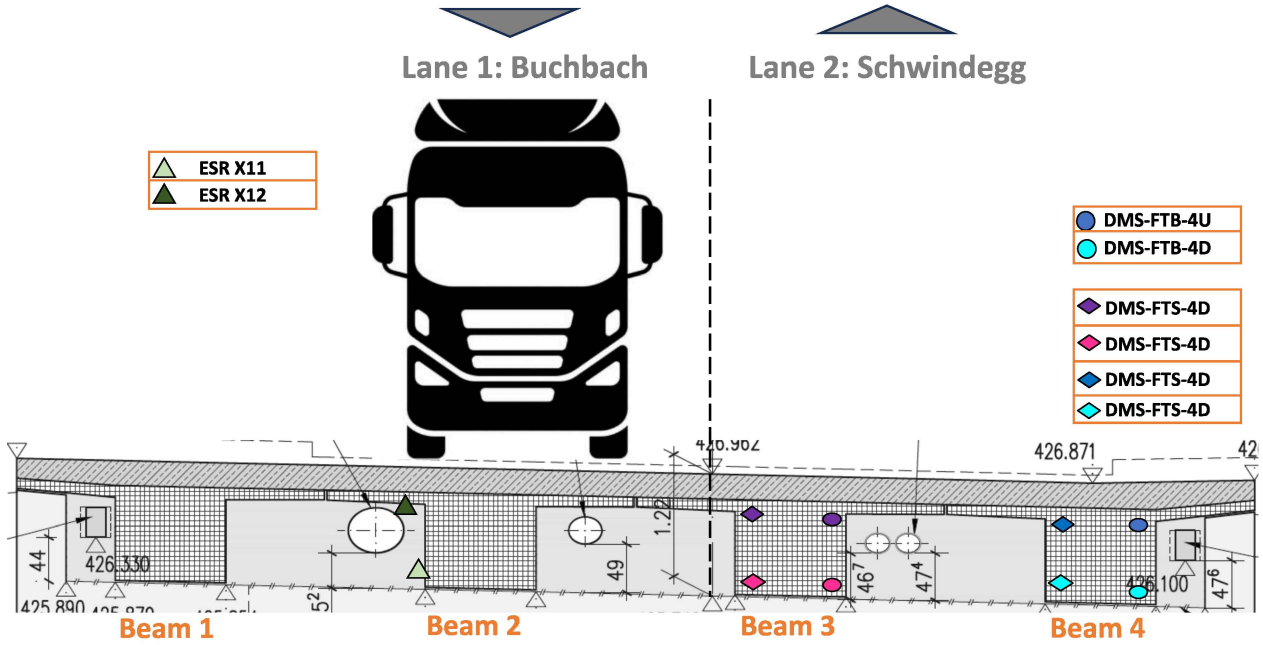

Figure 1: Cross section in mid span of the Isen bridge Schwindegg, showing the truck centered above Beam 2 and the arrangement of strain gauges (DMS) and Heidenhain ESR Sensors across the four girders

3.2 Test program

On April 15, 2025, a load testing program containing static and dynamic tests was carried out on the Isen Bridge to evaluate the sensor system under defined loading conditions. The test setup followed established principles for diagnostic load tests and formed part of a pilot study on digital twins for medium-span concrete bridges [6]. The objective was to generate strain responses at critical cross-sections to assess the plausibility of the sensor readings and the sensitivity of the structural model. For the preparation of the tests, the selection of test vehicles was based on the SLS to ensure that the bridge was not overloaded. The load level during tests with heavy vehicles should generally not exceed the service load limit, as this type of test setup does not include inherent structural safety [23]. The target test load was therefore limited to a maximum of 48 t.

Three trucks were used for the testing campaign: an unloaded 3-axle truck with a total weight of approximately 12.39 t (Truck 3), a fully loaded 3-axle truck (approx. 27.43 t, Truck 1), and a 5-axle semi-trailer truck (approx. 40.86 t, Truck 1). Bretschneider et al. emphasize that axle loads are particularly critical in load testing, as they significantly influence the structural response [23]. To precisely determine the truck weights during the calibration runs, a portable axle load scale was used. The tests were conducted for all three trucks. For the static tests, each vehicle was parked for ten minutes at midspan on both traffic lanes, as this point represents the location of maximum deflection in a single-span bridge. To ensure accurate vehicle positioning, the bridge centerline was determined using tape measurements at the expansion joints. The center of gravity (CoG) of each vehicle was calculated relative to the front axle. This allowed the CoG to be aligned with the structural center of the bridge, ensuring a consistent load distribution geometry. For the 3-axle truck, the CoG was determined to be at 2.819 m (loaded) and 2.345 m (unloaded); for Truck 2, it was located at 5.415 m.

For the dynamic tests, the vehicles crossed the bridge at constant velocities in both directions (Schwindegg to Buchbach and back) to ensure reproducible measurements. Based on previous research [16],[17],[33],[34], four speed levels were defined:

- **5 km/h**: walking speed for quasi-static reference conditions
- **20 km/h**: moderate dynamic effects
- **30 km/h**: increased dynamic excitation
- **50 km/h**: maximum allowable driving speed on site

Each test was carried out three times per lane. Trucks 1 and 2 were alternately deployed on separate lanes. After each passing, the trucks switched direction via designated turning points. A complete overview of the dynamic crossings, including braking tests and special scenarios such as pedestrian presence, is provided in Table 1. The table summarizes the number of passes per truck and lane, the corresponding speed ranges, and any special test conditions.

Table 1: Overview of dynamic calibration runs with vehicle weight, number of passes per lane, and comments

Truck No.	Weight	Lane 1	Lane 2	Comments
1	26 t	11 runs (5–50 km/h)	11 runs (5–46 km/h)	incl. braking and acceleration test
2	40 t	11 runs (5–40 km/h)	11 runs (5–40 km/h)	incl. braking test
3	11 t	13 runs (5–47 km/h)	13 runs (5–50 km/h)	incl. pedestrian presence on lane 2

Lane 1 corresponds in the northbound direction (towards Buchbach), and Lane 2 to the southbound direction (towards Schwindegg). Truck 1 and Truck 2 were operated simultaneously, alternating between lanes, while Truck 3 completed its runs individually. Notably, slightly higher final speeds were observed on Lane 2, possibly due to the longitudinal gradient of the bridge. Some runs also involved targeted braking maneuvers or additional load scenarios, such as the crossing of a pedestrian.

3.3 Test results

3.3.1 Plausibilisation of sensors

This subchapter focusses on the qualitative plausibility check of the structural response under varying influences, including environmental effects, static loading, and dynamic vehicle crossings. The analysis is based on strain gauges installed in between reinforcement layers and concrete elements. To suppress high-frequency noise while preserving structural response characteristics, a Savitzky–Golay filter was applied for thermal and quasi-static conditions. This filtering method, based on local polynomial regression (least squares), enables smoothing of strain signals without distorting relevant short-term events or long-term trends [35],[36]. For dynamic load effects, a Butterworth filter was used due to its flat frequency response in the passband, allowing precise separation of low- and high-frequency components without introducing ripple artifacts.

Regarding the environmental influence several strain gauges showed significant signal variation even before the vehicle loading. For instance, the weldable strain gauge DMS_FTS_3D recorded a continuous strain increase from approximately 1370 µm/m to 1401 µm/m between 07:10 and 08:20 (Figure 2). To explain this trend, external influences on the bridge must be considered. Since the beginning of the measurement in the morning, the temperature steadily increased. Additionally, there was intermittent sunshine. A more intense warming of the top side of the bridge compared to the bottom causes positive strain at the top of the cross-section (location of DMS_FTS_3U) and negative strain at the bottom (location of DMS_FTS_3D).

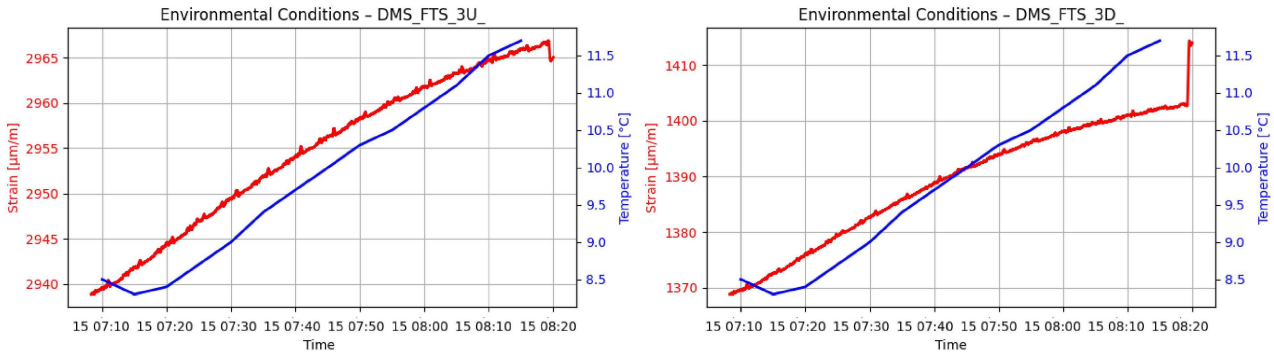

Figure 2: Environmental Conditions of strain gauge DMS_FTS_4D (Strain & Temperature)

Figure 3 shows the time series of strain measurements recorded during the first static load test. Sensor DMS_FTS_3U is positioned in the upper reinforcement layer at midspan, while DMS_FTS_3D is in the lower reinforcement. Truck 1 was positioned at midspan for ten minutes, first on Lane 1, then on Lane 2. The two loading phases are highlighted in the graph. During the first phase, all sensors showed a clear change in strain. After the truck was repositioned to Lane 2, which runs predominantly above beams 3 and 4, the recorded strain increased significantly. The more pronounced increase in strain observed during the second loading phase is attributed to the intensified bending effects caused by the position of the truck directly above the instrumented beams. The measured signals reflect both the structural location of the sensors and their mechanical coupling. DMS_FTS_3D is embedded in the lower reinforcement and responds to tensile strains, resulting in positive values under load. In contrast, DMS_FTS_3U is positioned in the upper

compression zone of the beam and therefore shows negative reactions. These results demonstrate the structural consistency of the bridge under the applied concentrated static load.

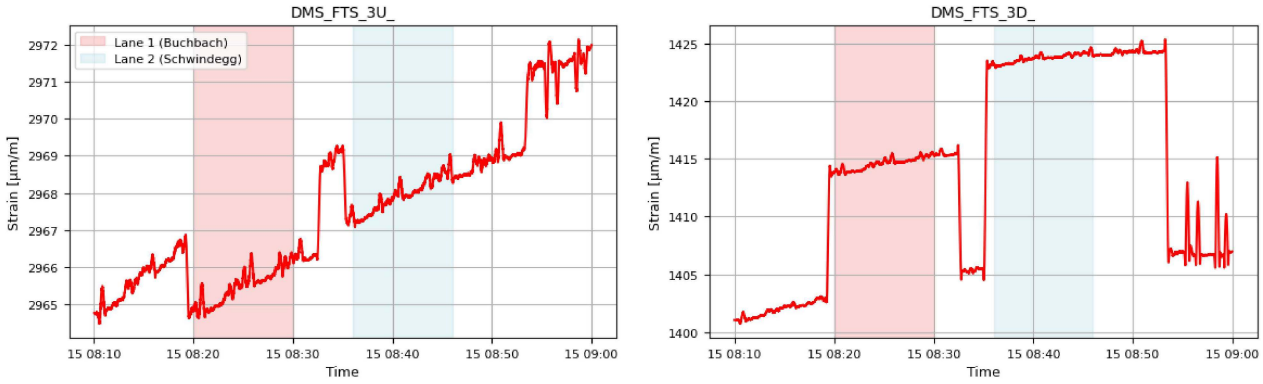

Figure 3: Filtered strain response of selected sensors during the first static load test with Truck 1 (27.43 t)

Between the two loading phases, the unloading of the structure due to the rearranging of the truck can be seen. The increase or decrease of the strain depends on the sensor location in the compression or tensile zone of the beam. These effects confirm not only the elastic behavior of the structure, but also the high responsiveness and reliability of the sensor system in capturing temporary unloading events. Additionally, a continuous strain drift is observed throughout the measurement period, which can be attributed to temperature effects. The measured strain during the static loading phases thus results from both the truck's load and the thermally induced expansion due to ambient warming. In the bottom of the beam, for instance at DMS_FTS_3D, traffic induced tensile strain and temperature induced compressive strain act in opposite directions, whereas in the top of the beam, as recorded by DMS_FTS_3U, both thermal expansion and load induced compression act in the same direction, leading to a cumulative effect.

During the dynamic truck passages, the sensors recorded short term changes in strain due to the crossing vehicles. The amplitudes of the dynamic peaks remain below the maximum values observed under static loading. Figure 4 shows the response of sensors DMS_FTS_3U (upper compression zone) and DMS_FTS_3D (lower tension zone) throughout the entire dynamic loading sequence. Particularly during the first two loading phases, a regular sequence of distinct impulses is observed, reflecting the rhythmic passage of the test vehicle. The signal from DMS_FTS_3U displays relatively uniform but low amplitude peaks, whereas DMS_FTS_3D reveals a more complex pattern with larger and more variable impulses.

Both sensors exhibit clearly different signal characteristics under dynamic and static loading. While static phases are characterized by flatter, plateau like curves without distinct impulses, the dynamic sequences consist of short term, rhythmically recurring strain events that correspond directly to the individual vehicle crossings. Figure 5 depicts the third dynamic load test, conducted under consistent boundary conditions using a single vehicle (Truck 1). A total of 26 crossings was recorded, alternating between Lane 1 and Lane 2, with gradually increasing speeds ranging from 5 km/h to approximately 50 km/h. The sensors DMS_FTS_3D and DMS_FTB_4D display a well-structured sequence of discrete peaks throughout this section.

In the signal of DMS_FTB_4D, each truck crossing appears as a clearly defined peak. The time intervals between successive peaks are nearly constant, corresponding to the regular timing of the test runs. Notably, the amplitudes vary depending on the lane: crossings on Lane 2, which runs closer to the beam, produce significantly stronger responses compared to those on Lane 1. This pattern is also visible in DMS_FTS_3D, though the overall amplitude levels are lower. The recorded strain patterns allow for a precise temporal and structural assignment of each loading event. The number, rhythm, and shape of the impulses match the documented test sequence with high accuracy. Variations in amplitude reflect both the spatial proximity of the sensors to the load application and their vertical position within the cross section.

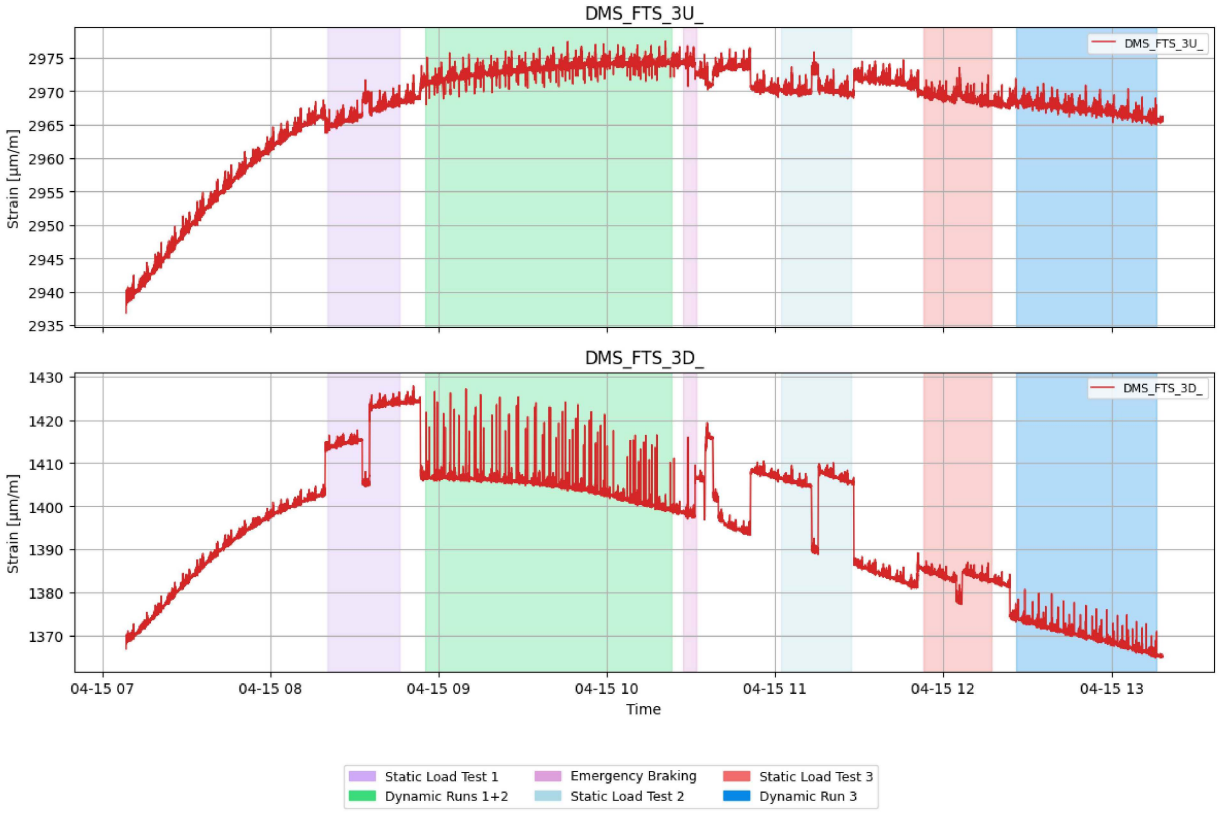

Figure 4: Strain in Reinforcement – Girder 3 (Top and Bottom Rebars).

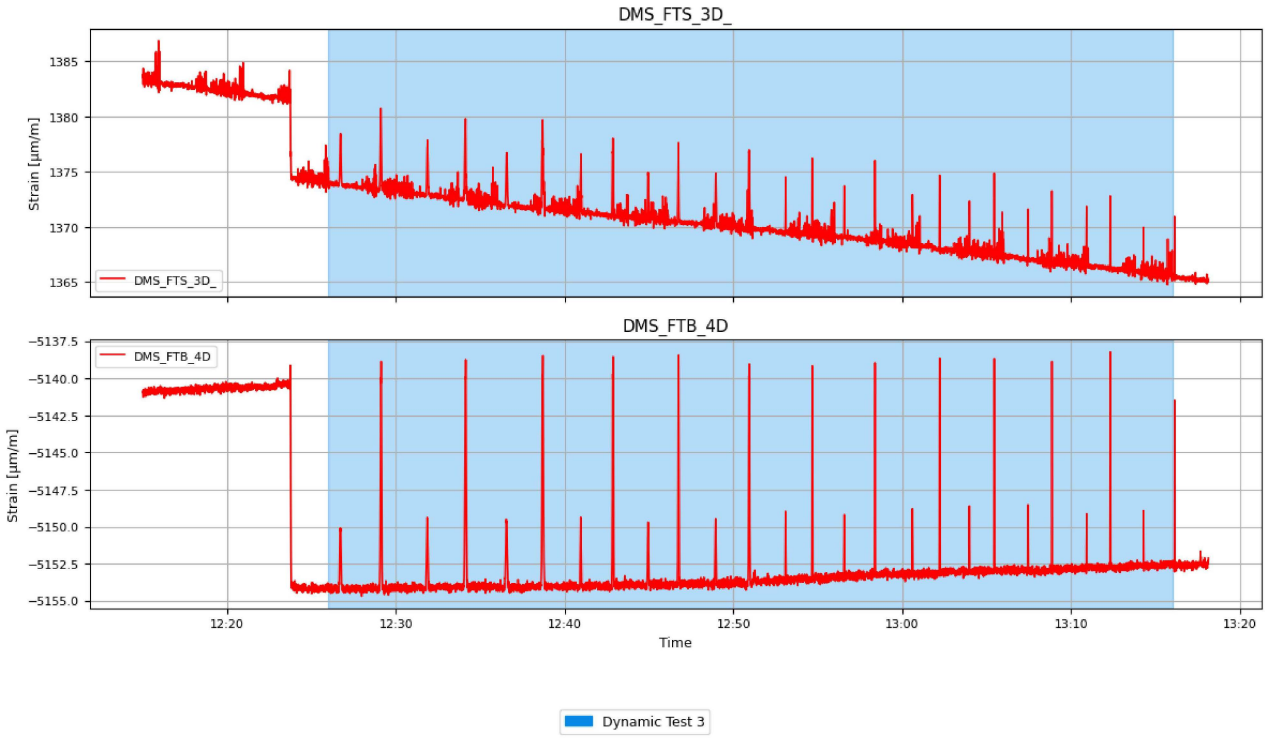

Figure 5: Zoomed-in analysis of Dynamic Test of Truck 3 with emphasis on DMS_FTS_3D_ and DMS_FTB_4D.

3.3.2 Validation of sensors using results from the statical calculation and data analysis

To determine the strain, a Butterworth filter was applied to the raw data from the calibration run in a first step. Figure 6 shows the measured strains on sensor X11. The red areas indicate the static tests, while the blue areas represent the dynamic truck crossings (analogue to Figure 4). The sensor was tared before starting the tests. The measurement results show a thermal induced decrease in strain values (see previous chapter). These effects are filtered out in a later step using a moving average filter. As an important finding, all crossings of the truck could be detected.

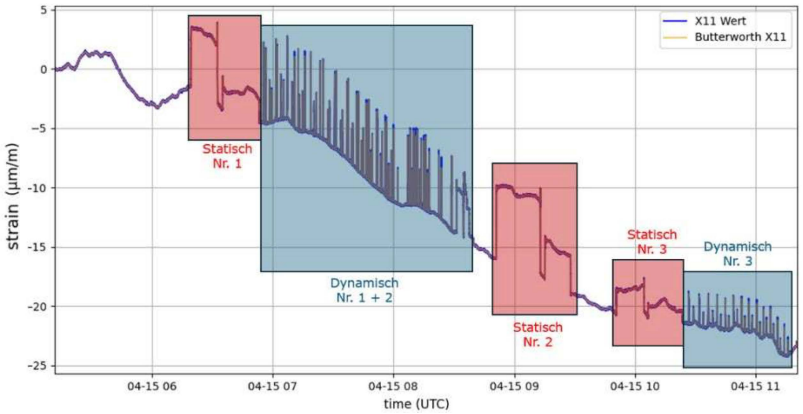

Figure 6: Measured strains on sensor X11 during static (red) and dynamic (blue) calibration tests on 15th April 2025

For comparison, the strain in the beam element is calculated based on the equations (1) and (2) and the structural data of the cross section, esp. geometry and material properties. The calculation is performed with a commercial software tool. The calculated strain change at the bottom of the cross-section under the quasi-permanent value of traffic loads, which equals approximately the load of the 3-axle calibration vehicle, is $\varepsilon = 0.093$ ‰ and the corresponding change in the concrete stress is $\sigma_c = 1{,}25\ MN/m^2$. As the average tensile stress of the concrete has not been exceeded, the bridge is in uncracked condition. The limit state of decompression is verified in the quasi-permanent situation for the project bridge. However, the calculated strain does not match the measured strain of the sensor X11 and is overestimated by a factor of 40 according to the calculation result.

To enable the correlation between strain and vehicle weights, calibration tests on the bridge are necessary, and the measured strains are assigned to the corresponding vehicle weights. Since the calculation of the strain did not yield sufficient consistency, the resulting bending moment is initially used to establish the link between the measurements and the computational model. Figure 7 shows the resulting bending moment distributions for the calibration vehicles. Due to the longer vehicle length of the heavier 5-axle semi-trailer, the bending moment does not increase linear with the vehicle weight. Especially for small to medium span bridges, this effect is more significant. As previously mentioned, variations also occur depending on the type of structural modeling. Although different structural models in various software solutions were created for the pilot bridge Schwindegg, the simple static model of a beam rigidly fixed on both ends will be used in this case.

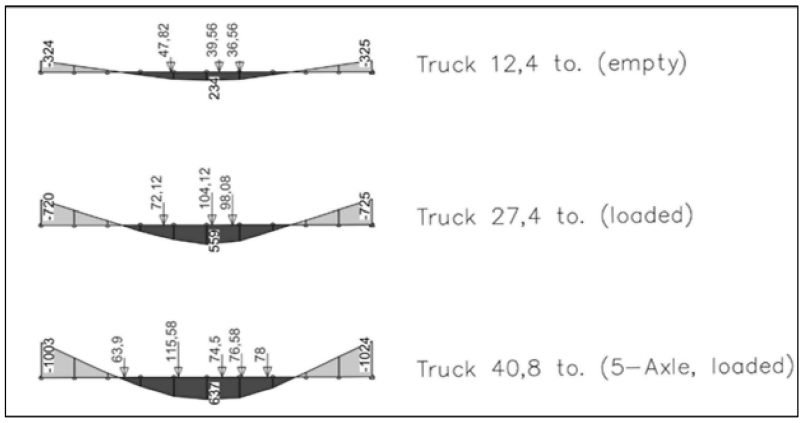

Figure 7: Resulting bending moments on a beam element analysis with the different calibration vehicle loads

As Figure 8 shows, the progression of the strains and bending moments follows the same qualitative trend with respect to the vehicle weight. The calculated values from the static model are single individual values, whereas the measured strains for the same vehicle with constant weight already show variations during the calibration test. As previously noted, during the calibration the different vehicles crossed the bridge several times with the same speeds. On the one

hand, a slight dependence on driving speed can be observed in the data and on the other hand, additional variations in the measurement data are visible, e.g. due to factors such as slight differences in the vehicle's lateral position within the driving lane or general measurement uncertainties.

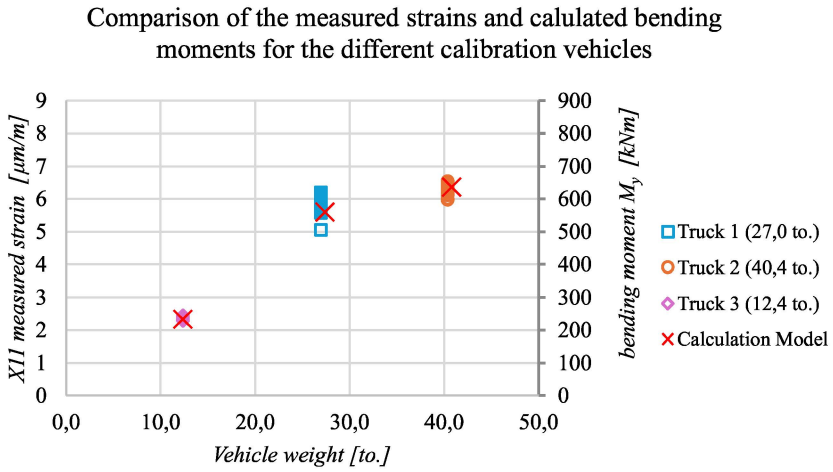

Figure 8: Comparison of the measured strains and calculated bending moments for the different calibration vehicles

3.3.3 Use of calibration tests for the traffic load determination

Based on the data from the pilot bridge project, an automated Python program was developed to analyse the available strain sensor data, determine daily maximum values, and generate extreme value distributions from these daily maxima for the measured traffic and determine the extrapolated maximum value over a service life of 50 years. Subsequently, temperature influences and self-weight effects are removed by pre-processing the data using a moving average over a 15-minute window. In Figure 9 the resulting maximum strain changes are visible.

The strains recorded by the X11 sensor during the use phase of the bridge can obviously be greater than those measured during the calibration test, since the actual heavy load traffic on the bridge is different from the limited number of vehicles used for calibration. Therefore, a model must be developed that can estimate vehicle weights corresponding to higher strain levels. This model should be conservative to ensure that vehicle weights are not underestimated. To derive a structure-specific load model from the obtained results, a comparison between the measured strains (or loads) on the bridge and the LM 1 load model is necessary. Using regression analysis, the theoretical equivalent weight of a vehicle corresponding to the LM 1 load is calculated. For the actual maximum strain value during the analyzed time span of 114 days this approach results in a utilization of 40% in comparison to the LM 1 load. When the (chosen) normal distribution is extrapolated over a 50-year service life, the utilization increases to 81%. These results once again highlight the value of a structure-specific assessment of the actual traffic loading on the bridge.

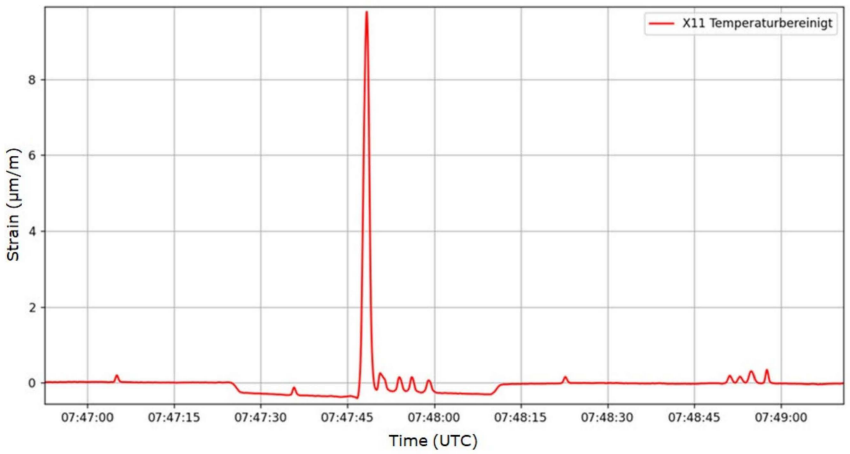

Figure 9: Maximum strain value after temperature compensation on 9th November 2024 around 07:48 am

To achieve more accurate results with this method, it would be beneficial to include data from the X12 sensor, which enables the identification of vehicle axle configurations. This allows for the determination of vehicle length and the conversion formula between strain and vehicle weight could then be supplemented with a "vehicle length factor". While there is the need for future work on this approach, Figure 10 shows that the five axles of the calibration are clearly

identifiable when measuring the strains of the concrete. However, it also becomes evident that this information is lost when analyzing only filtered data (Figure 10, yellow curve).

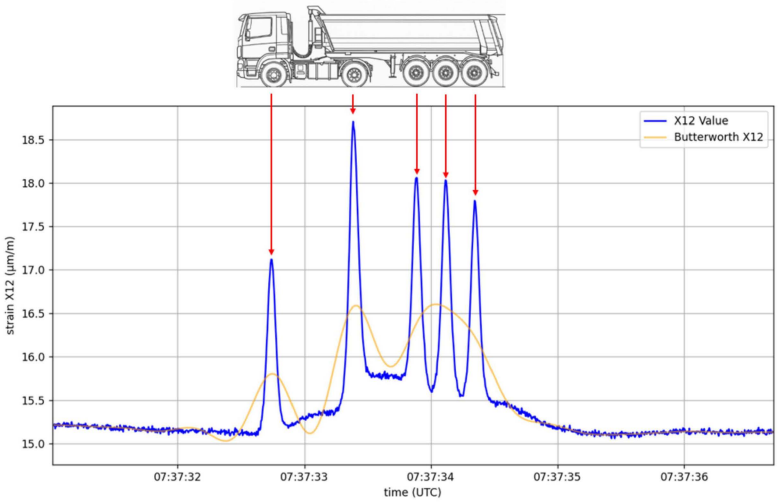

Figure 10: Measurement data from the X12 sensor during the crossing of the semi-trailer truck on 15th April 2025 showing the individual axles of the truck

4 Conclusion and Outlook

This paper shows why calibration is important for understanding the significance of a sensor on a bridge. After introducing the basics of structural health monitoring and load tests, the further processing of the measured data in physical simulation and data-driven analysis is presented. Using the example of the Isen Bridge Schwindegg (Germany) instrumented with sensors, the previous findings are applied and the results shown.

The conducted load testing campaign on the Isen Bridge provided essential insights into the structural behavior under controlled loading conditions and confirmed the reliability of the installed sensor system. The combination of static and dynamic tests enabled a differentiated analysis of strain development, temperature effects, and transient load response. The measured strain patterns corresponded well with the theoretical bending behavior of the beams, with tensile strains observed in the bottom flange and compressive strains in the top. Particularly noteworthy was the distinct signal quality during dynamic runs, where impulses could be clearly assigned to individual vehicle crossings. While some drift and variation in amplitude were observed, these are consistent with expected thermal and positioning effects. The test setup proved to be both efficient and transferable, requiring minimal structural intervention while allowing high resolution structural diagnostics. Overall, the approach demonstrated the potential of diagnostic testing for sensor validation and model calibration in the context of digital structural health monitoring.

There is a clear need for a realistic assessment of bridges, especially at the municipal level, since the normative load models are based on measurements on intensely used highway bridges and do not reflect the actual traffic loads experienced by many other bridges. A cost-effective approach to modify traffic load models for a more realistic assessment involves the targeted combination of measurement data with computational models. The uncertainty in the deduction of the measured strain and the corresponding vehicle weight is still needed to be further quantified. This includes factors such as the influence of vehicle speed, the condition or deterioration of the structure, cracking (in case of concrete without prestressing) and the choice of the structural model used to calculate the internal forces. Based on the presented case study, the possibility of a determination of the actual traffic loads based on measured strains is given. Furthermore, the platform for mapping digital twins is being developed to permanently execute and visualize these developed algorithms and manage the results.

Acknowledgements

This research project RISK.twin is funded by dtec.bw – Digitalization and Technology Research Center of the Bundeswehr which we gratefully acknowledge. dtec.bw is funded by the European Union – NextGenerationEU

5 References

[1] European Commission. Directorate General for Communications Networks, Content and Technology.: 2030 digital decade: report on the state of the digital decade 2023. Publications Office, 2023

[2] Federal Ministry for Economic Affairs and Climate Action: Digitalisation of the economy in Germany. Digitalisation index 2024. https://www.de.digital/DIGITAL/Redaktion/DE/Digitalisierungsindex/Publikationen/publikation-digitalisierungsindex-2024-kurzfassung-english.pdf?__blob=publicationFile&v=3, accessed 03-06-2025 (2024).

[3] Wimmer J., Braml T.: Digital twins for engineering structures—an industry 4.0 Perspective. Structural Concrete, **25**, 4202–4218, 2024, DOI: 10.1002/suco.202400683

[4] Farrar C. R., Worden K.: Structural Health Monitoring. A machine learning perspective. John Wiley & Sons, Ltd, Chichester, UK, 2012

[5] Wimmer J., Braml T.: Permanent structural health monitoring of a new prestressed concrete bridge. ce/papers, **6**, 691–700, 2023, DOI: 10.1002/cepa.2039

[6] Wimmer J., Braml T., Martinez R.: Digitale Zwillinge für Brücken mittlerer Stützweite – Pilotprojekt Brücke Schwindegg – Teil 1: Sensorik. Beton- Und Stahlbetonbau, **118**, 889–896, 2023, DOI: 10.1002/best.202300062

[7] Jaelani Y. et al.: Developing a benchmark study for bridge monitoring. Steel Construction, **16**, 215–225, 2023, DOI: 10.1002/stco.202200037

[8] Kainz C., Lapidus L., Braml T.: Modelling of traffic loads in a full-probabilistic reassessment of rural bridges based on measurement data – a case study. in 'Proceeding of the International Probabilistic Workshop', Vol 494, 197–208, 2024

[9] Schacht G., Bolle G., Marx S.: Belastungsversuche – internationaler Stand des Wissens. Bautechnik, **93**, 85–97, 2016, DOI: 10.1002/bate.201500097

[10] Moen C. D., Shapiro E. E., Hart J.: Structural analysis and load test of a nineteenth-century iron bowstring arch-truss bridge. Journal of Bridge Engineering, **18**, 261–271, 2013, DOI: 10.1061/(ASCE)BE.1943-5592.0000341

[11] Orbán Z., Gutermann M.: Assessment of masonry arch railway bridges using non-destructive in-situ testing methods. Engineering Structures, **31**, 2287–2298, 2009, DOI: 10.1016/j.engstruct.2009.04.008

[12] Lantsoght E. et al.: Proof load testing of reinforced concrete slab bridges in the Netherlands. Structural Concrete, **18**, 597–606, 2017, DOI: 10.1002/suco.201600171

[13] Nilimaa J. et al.: NSM CFRP strengthening and failure loading of a posttensioned concrete bridge. Journal of Composites for Construction, **20,** 2016, DOI: 10.1061/(ASCE)CC.1943-5614.0000635

[14] Puurula A. M. et al.: Assessment of the strengthening of an RC railway bridge with CFRP utilizing a full-scale failure test and finite-element analysis. Journal of Structural Engineering, **141,** 2015, DOI: 10.1061/(ASCE)ST.1943-541X.0001116

[15] TU Dresden: Load tests on the Elbe bridge in Bad Schandau with the participation of TU Dresden. https://tu-dresden.de/bu/bauingenieurwesen/imb/das-institut/news/belastungstests-an-der-elbbruecke-in-bad-schandau-gestartet?set_language=en, accessed 04-07-2025 (2025).

[16] Alampalli S. et al.: Bridge load testing: state-of-the-practice. Journal of Bridge Engineering, **26,** 2021, DOI: 10.1061/(ASCE)BE.1943-5592.0001678

[17] Lantsoght E. O.: Load testing of bridges. CRC Press, Leiden : CRC Press/Balkema, [2019] | Series: Structures and infrastructures series, ISSN 1747-7735, volumes 12-13, 2019

[18] Olaszek P., Łagoda M., Casas J. R.: Diagnostic load testing and assessment of existing bridges: examples of application. Structure and Infrastructure Engineering, **10**, 834–842, 2014, DOI: 10.1080/15732479.2013.772212

[19] Köhncke M., Jaelani Y., Mendler A., Neumann L., Wittenberg P., Rode-Klemm A., Keßler S.: Static and dynamic load tests on the bridge Vahrendorfer Stadtweg 2024

[20] Casas J. R., Gómez J. D.: Load rating of highway bridges by proof-loading. KSCE Journal of Civil Engineering, **17**, 556–567, 2013, DOI: 10.1007/s12205-013-0007-8

[21] Windmann S.: Intelligente brücke. Reallabor Intelligente Brücke im digitalen Testfeld Autobahn. Fachverlag NW in der Carl Ed. Schünemann KG, Bremen, 2022

[22] Deutsches Institut für Normung, Deutscher Ausschuss für Stahlbeton: DAfStb-Richtlinie Belastungsversuche an Betonbauwerken. Beuth Verlag GmbH, Berlin, 2000

[23] Bretschneider N. et al.: Technische Möglichkeiten der Probebelastung von Massivbrücken. Bautechnik, **89**, 102–110, 2012, DOI: 10.1002/bate.201100010

[24] Lubasch P.: Identifikation von Verkehrslasten unter Einsatz von Methoden des Soft Computing, Essen, 2009

[25] Schnellenbach-Held M., Karczewski B., Kühn O.: Intelligente Brücke - Machbarkeitsstudie für ein System zur Informationsbereitstellung und ganzheitlichen Bewertung in Echtzeit für Brückenbauwerke. Fachverlag NW, Bremen, 2014

[26] Nowak M., Fischer O., Müller A.: Realitätsnahe Verkehrslastansätze für die Nachrechnung der Gänstorbrücke über die Donau. Beton- und Stahlbetonbau, **115**, 91–105, 2020, DOI: 10.1002/best.201900060

[27] Nowak M. et al.: Verkehrsmonitoring an einer Autobahnbrücke – Datenerfassung zur lokalen Verkehrscharakteristik als Grundlage für objektspezifische Verkehrslastmodelle. Beton- und Stahlbetonbau, **118**, 636–648, 2023, DOI: 10.1002/best.202300043

[28] Steffens N., Geißler K.: Standortspezifisches ziellastniveau und objektspezifische Lastmodelle für die Nachrechnung auf der Basis von Bauwerksmonitoring. Bautechnik, **98**, 720–735, 2021, DOI: 10.1002/bate.202100051

[29] Röhling S., Meichsner H.: Rissbildungen im Stahlbetonbau. Fraunhofer IRB Verlag, 2018

[30] DIN EN 1991-2: Eurocode 1: Einwirkungen auf Tragwerke – Teil 2: Verkehrslasten auf Brücken, 2010

[31] Radusch P.: Ein Vorschlag für die baustatische Modellbildung von bestehenden Straßenbrücken in Massivbauweise für die Entwicklung objektspezifischer Verkehrslastmodelle am Beispiel der Brücke k-pa19 bei Kalteneck, Neubiberg, 2025

[32] Wimmer J., Braml T.: Geo-referenced localisation of SHM sensors on new bridge construction based on the example of the Digital Bridge Schwindegg (Germany). in 'Proceeding of the GJBS 2023. Osaka', 394–402, 2023

[33] Sanio D. et al.: Monitoring der Theodor-Heuss-Brücke – Teil 1 – Veranlassung, Monitoringkonzept und Erkenntnisse zum tragverhalten. Stahlbau, **91**, 172–183, 2022, DOI: 10.1002/stab.202100097

[34] Schartner M. et al.: Monitoring der Theodor-Heuss-Brücke – Teil 2 – Modellbildung und -verbesserung für messwertgestützte Ermüdungsnachweise. Stahlbau, **91**, 274–284, 2022, DOI: 10.1002/stab.202200005

[35] Niedźwiecki M. J. et al.: Application of regularized savitzky–golay filters to identification of time-varying systems. Automatica, **133**, 109865, 2021, DOI: 10.1016/j.automatica.2021.109865

[36] Schafer R.: What is a savitzky-golay filter? [lecture notes]. IEEE Signal Processing Magazine, **28**, 111–117, 2011, DOI: 10.1109/MSP.2011.941097